

Do Proteins at Low Temperature Behave as Glasses? A Single-Molecule Study

Jürgen Baier,[†] Martin F. Richter,[†] Richard J. Cogdell,[‡] Silke Oellerich,[†] and Jürgen Köhler^{*,†}

Experimental Physics IV and BIMEF, University of Bayreuth, 95440 Bayreuth, Germany, and Division of Biochemistry and Molecular Biology, Institute of Biomedical and Life Sciences, Biomedical Research Building, University of Glasgow, 120 University Place, Glasgow G12 8TA, U.K.

Received: November 10, 2006; In Final Form: December 7, 2006

We have recorded long spectral diffusion trajectories from individual LH2 pigment–protein complexes from the purple bacterium *Rhodobacter sphaeroides* at 1.4 K. From these data, the spectral cumulants of the absorption lines of individual, protein-embedded BChl *a* pigments have been evaluated. It appears that the first and second cumulants cannot be described by the predictions of the well tested standard two-level system (TLS) model for spectral diffusion in glasses. The results of the present study clearly show that there is a fundamental difference between the relaxation behavior of our test protein and that of glasses.

Introduction

Commonly, polymers and glasses display a rugged potential energy surface,^{1–3} which directly reflects their structural disorder. In such systems, structural dynamics is supposed to only occur in spatially localized regions that are characterized by double well potentials. Since, at low temperatures, only the energetically lowest states are occupied, these potentials can be approximated as two-level systems (TLSs),^{4–6} whose energies and tunneling matrix elements are randomly distributed. For example, the temperature dependence of the heat capacity of glasses and glasslike materials can be explained successfully with this model.⁷ The influence of the TLSs can be made visible by optical spectroscopy because the exact energies of the electronically excited states of chromophores, that is, molecular reporters, embedded in the amorphous host matrix are fine-tuned by the interaction with their local surroundings. Consequently, if the local environments of the chromophores are not static but show temporal fluctuations, that is, flipping of TLSs, the absorption frequencies of the chromophores undergo temporal fluctuations as well.^{8–10} In hole-burning experiments,^{11,12} where the observed fluctuations are averaged over the ensemble of chromophores in resonance with the laser frequency, these fluctuations are manifested as waiting time dependent line broadening. In single-molecule experiments, these fluctuations can be directly observed^{10,13,14} and lead to random line shapes,¹⁵ which are determined by the mutual relationship between the experimental time that is required to record a single-molecule spectrum and the time scale of the spectral diffusion processes.¹⁶ The problem of random line shapes of single molecules embedded in disordered hosts is related to Lévy statistics, reflecting the long-range interaction between the TLSs and the single molecule.¹⁷ For glasslike hosts that are commonly described by the standard TLS model, the predictions of the Lévy formalism have been impressively verified by the Kador group.¹⁸

Proteins also feature a rugged energy landscape.^{3,19,20} They are heteropolymers, which, though they usually have structures well enough ordered to allow their determination by methods such as X-ray crystallography, are often required to be rather flexible in order to discharge their biological functions. Indeed, this is why there is so much interest in studying protein structure dynamics. These structural fluctuations can be rapid at room temperature and introduce a microscopic randomness, and thus, it is not surprising therefore that their behavior has often been likened to that of a glass.²¹

Working at cryogenic temperatures, the various protein substructures are separated by a static distribution of barriers, which effectively trap the biomolecule in distinct physical states. Moreover, the time scales of these fluctuations are shifted into a range that is experimentally accessible.^{22,23} This then offers the opportunity to directly study the detailed organization of the protein's energy landscape. At low temperatures, frozen solutions of proteins appear structurally random (at least on a microscale), homogeneous, and isotropic, for example, glasslike. Indeed, at low temperatures, the specific heat of proteins follows a quasi-linear behavior as a function of temperature, which is also a signature of a glass.²⁴ On the other hand, many experiments on heme proteins have demonstrated unambiguously that the dynamic laws that govern their spectral diffusion are different in proteins from that in glasses.²⁵ Hence, it was an obvious question as to whether the interplay of organization and randomness, which is a particular feature of proteins, leads to novel features in the structural dynamics of proteins in comparison to glasses.

Here, we address this issue by single-molecule spectroscopy by observing the protein dynamics of individual light-harvesting 2 (LH2) complexes from *Rhodobacter (Rb.) sphaeroides*, strain 2.4.1. Briefly, LH2 is a pigment–protein complex that serves as a peripheral light-harvesting antenna in bacterial photosynthesis. The structure of this complex has been obtained by an electron microscopy projection map with 6 Å resolution²⁶ and features a highly symmetric assembly that comprises 27 bacteriochlorophyll *a* (BChl *a*) molecules arranged in two concentric rings. One ring consists of a group of nine well-separated BChl *a* molecules (B800) absorbing light at about 800 nm (12 500 cm^{−1}). The other ring consists of 18 closely

* Corresponding author. Address: Experimental Physics IV and BIMEF, University of Bayreuth, Universitätsstrasse 30, 95440 Bayreuth, Germany. Phone: +49(0)921-55-4001. Fax: +49(0)921-55-4002. E-mail: Juergen.koehler@uni-bayreuth.de.

[†] University of Bayreuth.

[‡] University of Glasgow.

interacting BChl *a* molecules (B850), which absorb at about 850 nm (11 765 cm^{-1}). In this contribution, we focus on the spectroscopy of the B800 chromophores, which are ideally suited to act as probes to monitor changes in their local protein environment. In order to obtain information about the protein dynamics, long series of B800 fluorescence–excitation spectra from individual LH2 complexes were recorded. The data were analyzed by a spectral moment and cumulant analysis, which yielded distributions of the generalized spectral positions and line widths for the observed optical transitions of the protein-embedded chromophores. In contrast to previous hole-burning studies, this approach allows one to distinguish between contributions to spectral diffusion that stem from fluctuations of the spectral position and those from fluctuations of the line width, thus providing unequivocal information for comparison with theoretical predictions.

Experimental Methods

LH2 complexes of *Rb. sphaeroides* were prepared as described previously.²⁷ The samples for single-molecule spectroscopy were prepared by spin-coating a highly diluted solution of detergent-solubilized LH2 onto a lithium fluoride substrate and subsequently cooled down to 1.4 K in a helium-bath cryostat. As described in detail in ref 28, individual complexes were then excited by circularly polarized light from a continuous wave tunable titanium:sapphire laser in the spectral range 780–820 nm and the fluorescence was detected by an avalanche photodiode (SPCM-AQR-16, EG&G). The laser was scanned repeatedly over this spectral region with a scan speed of 44 cm^{-1}/s . Long series of 1000–2000 spectra were recorded for five different complexes, with three different excitation intensities (5, 10, and 15 W/cm^2).

Results and Discussion

An example of a long series of fluorescence–excitation spectra is shown in Figure 1A (top) in a two-dimensional representation, where the horizontal axis corresponds to the photon energy, the vertical axis corresponds to time (i.e., number of scans), and the grayscale corresponds to the absorption intensity. This sequential data acquisition scheme reveals the temporal evolution of the absorption lines of the individual B800 pigments as spectral trails. Interestingly, distinctively different spectral diffusion behaviors can be observed for the individual absorption lines. Averaging over all individual scans results in a sum spectrum, which is shown in Figure 1A (bottom). Figure 1B shows an expanded view of some individual scans of the spectral feature boxed in Figure 1A together with a Lorentzian (solid line) that has been fitted to the absorption profile. These spectra clearly demonstrate that both the spectral position and the width of an individual absorption line vary with time. As evidenced by Figure 1B, the signal-to-noise ratio of the individual spectra is sufficient to obtain the line widths with an accuracy that is determined by the spectral resolution of the setup ($\approx 1 \text{ cm}^{-1}$). The respective width distribution of the absorption line boxed in Figure 1A is shown in Figure 2. It peaks at about 4 cm^{-1} and displays a width of 8 cm^{-1} . This is in agreement with the general observation that absorption lines of single molecules embedded in disordered matrices can have complex shapes, so that a description with a single line width is not sufficient.¹⁵

As a prerequisite for the analysis, individual molecular absorption lines were chosen that were well separated from the absorption lines of other pigments in the studied pigment–protein complexes. This selection does not bias the analysis,

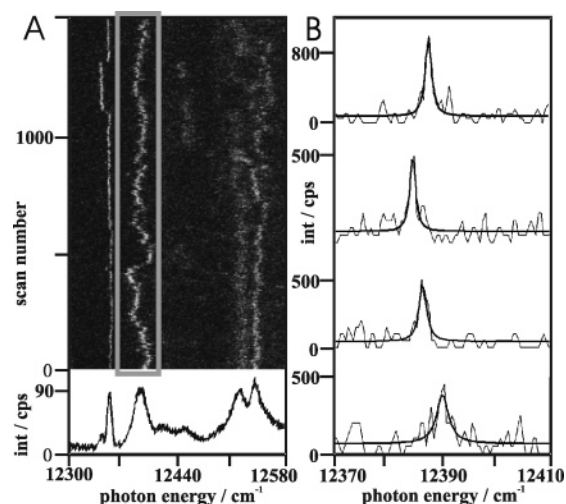


Figure 1. (A) (top) Two-dimensional representation of 1500 fluorescence–excitation spectra of the B800 band of an individual LH2 complex from *Rb. sphaeroides* measured at a temperature of 1.4 K. The horizontal axis corresponds to the laser-excitation energy, the vertical axis corresponds to the time and scan number, and the fluorescence intensity is given by the grayscale. The spectra were recorded with an excitation intensity of 10 W/cm^2 . (bottom) Average over all 1500 fluorescence–excitation spectra. (B) Single fluorescence–excitation spectra of the spectral feature boxed in part A of the figure on an expanded scale together with Lorentzian fits (solid line). The intensity of the individual spectra is given in counts per second (cps) and refers to the number of detected photons.

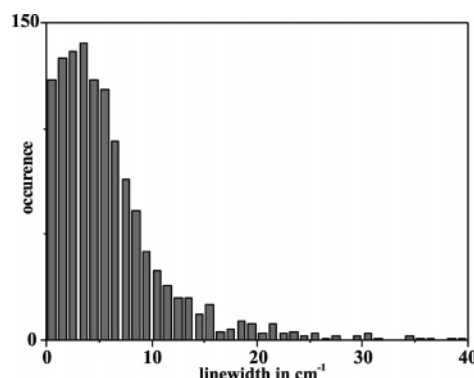


Figure 2. Distribution of the line width for the absorption line marked in Figure 1. The line width was determined by fitting for each scan a Lorentzian to the measured absorption line.

since all complexes studied here displayed an uncorrelated spectral diffusion behavior of the individual pigments, indicating hardly any interactions between them. For all absorption lines from individual B800 pigments that have been studied, we observe a distribution of line widths. In order to estimate the effect of light-induced line width broadening, we studied the complexes at three different excitation intensities (5, 10, and 15 W/cm^2). The resulting line width distributions showed essentially the same result, indicating that, at the temporal resolution of our experiment, the distribution of the line widths is not affected by light-induced spectral diffusion.

As shown previously by Barkai et al.,¹⁸ a useful set of parameters to describe irregular line shapes are spectral moments. For a discrete data set, these central moments are defined by

$$M_1 = \frac{1}{n} \sum_i \nu_i I_i \quad \text{with} \quad n = \sum_i I_i \quad (1)$$

and

$$M_2 = -\frac{1}{n} \sum_i (\nu_i - M_1)^2 I_i \quad (2)$$

with $M_{1,2}$ being the first (M_1) and second (M_2) spectral moments, I_i the fluorescence intensity at spectral position i , and ν_i the photon energy at this spectral position. n is the sum of the intensity of the complete spectrum. The first spectral moment is a measure for the spectral center of mass, and the second moment is a generalized measure for the line width of the feature. For analytical calculations, however, the moments are often not suited. Rather than using spectral moments, it is better to use spectral cumulants,¹⁸ which can be calculated from the spectral moments recursively as

$$K_1 = M_1 - M_0 \quad (3)$$

and

$$K_2 = M_2 - \frac{K_1^2}{(M_1 - M_0)^2} \quad (4)$$

where M_0 denotes the vacuum transition frequency and K_1 and K_2 the first and second cumulants. As shown in ref 29, M_0 can be approximated by the spectral mean position of the spectral feature under study. The first cumulant is a measure for the deviation of the spectral position of the observed chromophore from the spectral mean position of the spectral feature under study, while the second cumulant is a generalized measure for the transition line width of the chromophore. The analysis, which was applied to 14 absorption lines, yields a set of two moments and two cumulants for each spectral feature of a single spectrum. The standard TLS model predicts a Lorentzian-shaped distribution for the first cumulant

$$P(K_1) = \frac{1}{\pi} \frac{z_1}{K_1^2 + z_1^2} \quad (5)$$

and a Smirnoff distribution

$$P(K_2) = \frac{2}{\sqrt{\pi} z_{1/2}^2} \left(\frac{z_{1/2}}{2K_2} \right)^{3/2} \exp\left(-\frac{z_{1/2}^2}{2K_2}\right) \quad (6)$$

for the second cumulant.¹⁷ The parameters z_1 and $z_{1/2}$ are fit parameters that are specific for the two distribution functions. We want to note that the calculation of the cumulants does not require any fitting procedure. However, it is important to choose an appropriate discrimination threshold with respect to the background noise level for the analysis. A detailed stability analysis is given in ref 15.

As an example, the application of the cumulant analysis to 1500 spectra taken of the absorption line marked in Figure 1 is presented in detail in Figure 3. The analysis yields the first and second spectral moments (Figure 3A,B) and cumulants (Figure 3C,D), respectively, of each spectrum taken of the absorption line; that is, each histogram contains 1500 data points. Fitting the probability distributions of the cumulants given by eqs 5 and 6 to the experimentally obtained distribution of the first and second cumulants (Figure 3C,D), we obtain the dashed curves plotted in the corresponding histograms (Figure 3C,D). The agreement between the experimental and theoretical distributions is obviously dissatisfactory. Actually, the distribution of the first cumulant for all studied absorption lines features

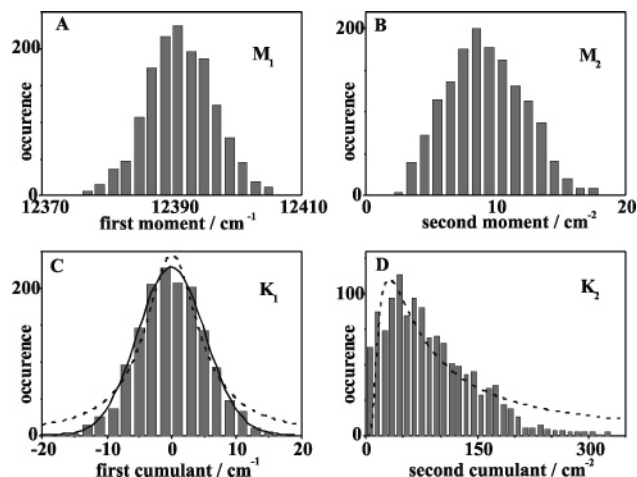


Figure 3. Distribution of the (A) first spectral moment, (B) second spectral moment, (C) first spectral cumulant, and (D) second spectral cumulant. The results are based on the analysis of the molecular absorption line marked in Figure 1. The dashed lines in parts C and D, respectively, represent the fit results based on eqs 5 and 6, which yielded $z_1 = 5.0 \text{ cm}^{-1}$ and $z_{1/2} = 9.6 \text{ cm}^{-1}$. The full line in part C corresponds to a Gaussian with a width of 10.3 cm^{-1} (fwhm).

a Gaussian rather than a Lorentzian shape, as evidenced by the full line in Figure 3C. This clearly illustrates that especially the distribution of the first cumulant does not obey the predictions of the standard TLS model. Since the calculation of the first cumulant is very robust for a wide range of signal-to-noise ratios of the analyzed spectra,¹⁵ this is an observation of particular importance. The discrepancy between the experimentally obtained cumulant distributions and the theoretical predictions based on the standard TLS model is in clear contrast to single-molecule experiments performed on chromophores embedded in a glassy matrix, which have shown an excellent agreement between the distribution of cumulants extracted from the experimental data and the theoretical predictions.¹⁸

Thus, our results clearly show that the spectral dynamics behavior of individual protein-embedded chromophores cannot be described by the standard TLS model. Doubts that the standard TLS model does provide an appropriate frame for the description of the spectral dynamics of chromophores embedded in proteins have been raised already from hole-burning experiments on small water-soluble proteins by Friedrich and co-workers.^{25–27} This work was performed on heme proteins with an altered chromophore to allow for optical spectroscopy. In contrast, the results reported here have been obtained by probing directly the contributions to the spectral diffusion of a chromophore that is naturally embedded in a transmembrane protein. Despite the differences in the experimental techniques and the distinctively different types of proteins, these results can be taken as a clear indication that the spectral dynamics behavior of proteins can in general not be described by the standard TLS model.

Conclusions

In summary, the analysis of our data obtained by single-molecule spectroscopy allows us to conclude that a unified description of the main dynamic features of spectral diffusion of proteins on one hand and polymers and glasses on the other hand is not appropriate. Our results show that proteins at low temperature do not behave glasslike and that the conformational fluctuations of proteins cannot be described by the standard TLS model.

Acknowledgment. R.J.C. thanks BBSRC for financial support. S.O. acknowledges a MC reintegration grant from the EU. We thank Lothar Kador for fruitful discussions.

References and Notes

- (1) Onuchic, J. N.; Luthey-Schulten, Z.; Wolynes, P. G. *Annu. Rev. Phys. Chem.* **1997**, *48*, 545–600.
- (2) Bryngelson, J. D.; Onuchic, J. N.; Succi, N. D.; Wolynes, P. G. *Proteins: Struct., Funct., Genet.* **1995**, *21*, 167–195.
- (3) Frauenfelder, H.; Wolynes, P. G.; Austin, R. H. *Rev. Mod. Phys.* **1999**, *71*, S419–S429.
- (4) Anderson, P. W.; Halperin, B. I.; Varma, C. M. *Philos. Mag.* **1972**, *25*, 1–9.
- (5) Phillips, W. A. *J. Low Temp. Phys.* **1972**, *7*, 351–360.
- (6) Suarez, A.; Silbey, R. J. *J. Phys. Chem.* **1994**, *98*, 7329–7336.
- (7) Phillips, W. A. *Rep. Prog. Phys.* **1987**, *50*, 1657–1708.
- (8) Moerner, W. E.; Basché, Th. *Angew. Chem., Int. Ed.* **1993**, *32*, 457–476.
- (9) Moerner, W. E.; Plakhotnik, T.; Irngartinger, Th.; Croci, M.; Palm, V.; Wild, U. P. *J. Phys. Chem.* **1994**, *98*, 7382–7389.
- (10) Zumbusch, A.; Fleury, L.; Brown, R.; Bernard, J.; Orrit, M. *Phys. Rev. Lett.* **1993**, *70*, 3584–3587.
- (11) Völker, S. *Ann. Rev. Phys. Chem.* **1989**, *40*, 499–530.
- (12) Maier H.; Kharlamov, B.; Haarer, D. *Tunneling systems in amorphous and crystalline solids*; Springer: Berlin, 1998; pp 317–387.
- (13) Fleury, L.; Zumbusch, A.; Orrit, M.; Brown, R.; Bernard, J. *J. Lumin.* **1993**, *56*, 15–28.
- (14) Ambrose, W. P.; Moerner, W. E. *Nature* **1991**, *349*, 225–227.
- (15) Naumov, A. V.; Vainer, Yu. G.; Bauer, M.; Kador, L. *J. Chem. Phys.* **2002**, *116*, 8132–8138.
- (16) Plakhotnik, T.; Donley, E. A.; Wild, U. P. *Ann. Rev. Phys. Chem.* **1997**, *48*, 181–212.
- (17) Barkai, E.; Silbey, R.; Zumofen, G. *Phys. Rev. Lett.* **2000**, *84*, 5339–5342.
- (18) Barkai, E.; Naumov, A. V.; Vainer, Yu. G.; Bauer, M.; Kador, L. *Phys. Rev. Lett.* **2003**, *9107*, 5502.
- (19) Frauenfelder, H.; Sligar, S. G.; Wolynes, P. G. *Science* **1991**, *254*, 1598–1603.
- (20) Nienhaus, G. U.; Young, R. D. *Encycl. Appl. Phys.* **1996**, *15*, 163–183.
- (21) Iben, E. T.; Braunstein, D.; Doster, W.; Frauenfelder, H.; Hong, M. K.; Johnson, J. B.; Luck, S.; Ormos, P.; Schulte, A.; Steinbach, P. J.; Xie, A. H.; Young, R. D. *Phys. Rev. Lett.* **1989**, *62*, 1916–1919.
- (22) Hofmann, C.; Aartsma, T. J.; Michel, H.; Köhler, J. *Proc. Natl. Acad. Sci. U.S.A.* **2003**, *100*, 15534–15538.
- (23) Schlichter, J.; Friedrich, J.; Herenyi, L.; Fidy, J. *J. Chem. Phys.* **2000**, *112*, 3045–3050.
- (24) Jankowiak, R.; Hayes, J. M.; Small, G. M. *Phys. Rev. B* **1988**, *38*, 2084–2088.
- (25) Fritsch, K.; Friedrich, J.; Leeson, D. T.; Wiersma, D. A. *J. Phys. Chem. B* **1997**, *101*, 6331–6340.
- (26) Walz, T.; Jamieson, S. J.; Bowers, C. M.; Bullough, P. A.; Hunter, C. N. *J. Mol. Biol.* **1998**, *282*, 833–845.
- (27) Hofmann, C.; Aartsma, T. J.; Michel, H.; Köhler, J. *New J. Phys.* **2004**, *6*, 1–15.
- (28) Lang, E.; Baier, J.; Köhler, J. *J. Microsc.* **2006**, *222*, 118–123.
- (29) Barkai, E.; Naumov, A. V.; Vainer, Yu. G.; Bauer, M.; Kador, L. *J. Lumin.* **2004**, *107*, 21–31.